Nawfal A. Noori
Kadhim A. Aadim

Department of Physics,
College of Science,
University of Baghdad,
Baghdad, IRAQ

Spectroscopic Analysis of Aluminum Plasma Produced by DC Magnetron Sputtering Technique

This study explores the influence of argon pressure and applied voltage on plasma characteristics in a DC magnetron sputtering system. The discharge was created at working vacuum pressures ranging from 0.05 to 0.4 mbar using different applied voltages from 400 to 1200 V to investigate the relations between these parameters and emission intensities to predict the optimum point of sputtering efficiency of aluminum. The optimal working pressure was 0.3 mbar at the highest emission intensities of both sputtering gas and metal atoms, indicating maximum sputtering rate. Increasing the applied voltage caused higher emission intensity due to increasing energy delivered to the charged particles, leading to more ionization and excitation collisions. Plasma parameters comprising electron number density, electron temperature, plasma frequency, Debye length, and Debye number appeared to be related to working pressure and voltage. These study outcomes offer a valuable strategy for adjusting sputtering processes by fine-tuning working pressure and applied voltage while observing the characteristics of induced plasma.

***Keywords*:** DC discharge; Plasma parameters; Optical emission spectroscopy; sputtering
Received: 26 November 2024; **Revised:** 19 January 2025; **Accepted:** 26 January 2025

1. Introduction

DC magnetron sputtering is a physical vapor deposition method for depositing high-quality thin films. In this technique, a metal or semiconductor target is bombarded with high-energy positive ions, often argon ions, in a low-pressure ejecting the target material and deposited onto a substrate [1-3]. DC magnetron sputtering has a wide range of applications in electronics and optics [4,5]. Nanoparticles can be prepared using plasma by different techniques such as pulsed laser ablation [6-8], plasma jet, and magnetic sputtering [9-11].

The properties of the sputtered films can be tuned by controlling the plasma characteristics related to these properties. Optical emission spectroscopy (OES) is one of the most critical monitoring techniques due to its ease and the possibility of applying it outside the chamber without affecting the plasma properties [12]. OES provides real-time monitoring of the changes that occur during the sputtering process by analyzing the light emitted from the plasma, which allows adjustments to the operating parameters and adjusts the deposition process [13]. This technique provides detailed spectral information, such as the plasma components of the species and their ratios, which ensures optimal film properties [14]. Using OES, the interactions among atoms and ions can be explained, giving details about their energy, concentrations, and compositions [15].

Held et al. [16] investigated sputtering from solid and liquid phases to prepare Al films. The deposition rates of sputtering with pulsed power were studied. The OES shows the composition of the sputtered ions in the gas phase. The reliance on grain sizes and sputtering factors was investigated. Sidelev et al. [17] studied the ionization manner of sputtered atoms in magnetron sputtering of Ti, Cr, and Al targets using optical emission spectroscopy of spatial emission to trace the optimum ionization location. Most Ti atoms were ionized within 0.5 mm from the target, whereas sputtered Al or Cr travel further before ionization happens [18-22].

This article explores the advantages of employing OES as a robust in DC magnetron sputtering, exploring how different working conditions, including working pressure and applied voltage, influence plasma parameters and, consequently, the optimum working parameter for deposited aluminum films using DC magnetron sputtering and efficiency of thin film deposition processes.

2. Experimental Setup

A DC magnetron sputtering system with an aluminum target of 8 cm in diameter and a 5 cm inter-electrode distance with a closed-field magnetron is utilized. The sputtering system is illustrated schematically in Fig. (1). The discharge produced inside a vacuum glass chamber, as shown in Fig. (1), was evacuated firstly to a base pressure of 10^{-6} mbar, using rotary and diffusion pumps, and then to working pressure at different levels of 0.05, 0.1, 0.2, 0.3, and 0.4 mbar through injection of argon gas by a needle valve. The vacuum level was monitored using Pirani and Penning gauges. The discharge was achieved using different applied voltages across the electrodes. A Thorlabs CCS100/M spectrometer was employed to diagnose the plasma characteristics, employing the spectral within the 200-1000 nm range for a point near the cathode. The data on plasma characteristics with varying vacuum pressures and applied voltages were analyzed to study plasma behavior at these conditions.

Vol. 21, No. 2, April-June 2025, pp. 191-198

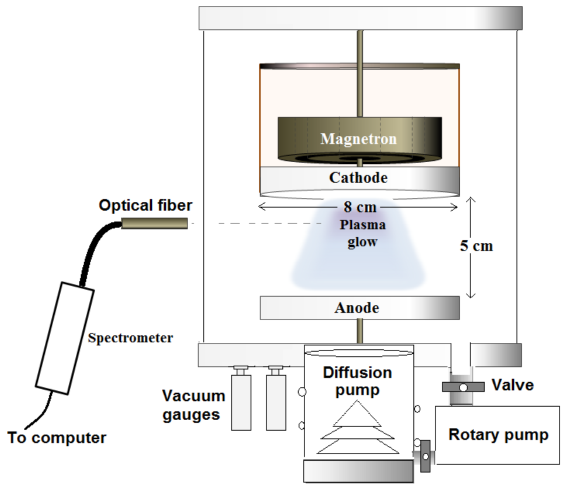

Fig. (1) Scheme of DC magnetron discharge system and the optic fibre location of spectrometer

3. Results and Discussions

Figure (2) shows the spectroscopic patterns of plasma emissions generated throw breakdown in argon using a DC-magnetron sputtering system from an aluminum target at varied working pressures of 0.05, 0.1, 0.2, 0.3, and 0.4 mbar and maintained applied voltage of 1200 V. According to the NIST database, The observed emissions correlated with standard emissions corresponding to electronic transitions in atomic and ionic Al and Ar [23]. Most emissions of atomic species corresponding to ionic ones suggest low ionization levels within the plasma environment [24]. Notably, different emission lines displayed varying intensity ratios between different emissions at various pressures, where the difference in pressure causes a difference in plasma temperature. This difference in temperature causes a difference in particle population into energy states, consequently yielding more intense emission lines. This trend is consistent with the Boltzmann distribution [21].

Moreover, the variation in working pressures revealed variation in general emission intensities. The emission line intensities were increased with increasing working pressure from 0.05 mbar up to 0.3 mbar. This increment in intensity is due to the increase in the cross-section of excitation collisions and subsequent emission processes [22]. However, the operational pressure increased to 0.4 mbar, and an inverse trend was observed. Increasing electron collision within the plasma with a process called "collisional quenching". In this process, highly energetic electrons come upon collisions that result in energy dissipation, preventing reaching the excitation or ionization threshold [23]. The higher collision rate causes an inverse trend of reducing the excitation and ionization process.

Figure (3) displays the emission spectra from breakdown plasma in argon using DC magnetron sputtering using an aluminum target at fixed working pressures of 0.3 mbar at different applied voltages 400, 600, 800, 1000, and 1200 V. The spectral lines were related to atomic and ionic emissions for gas and the sputtered metal species (Ar I, Al I, Ar II, and Al II) with the NIST database. Also, the atomic more distinctive than ionic emissions suggests low ionization levels [20]. Generally, increased applied DC voltage led to enhanced emission line intensities due to the acceleration of charged particles. Consequently, higher electron energies increased the probability of excitation collisions, resulting in a high population rate of particles of high energy and, afterward, higher emission line intensities.

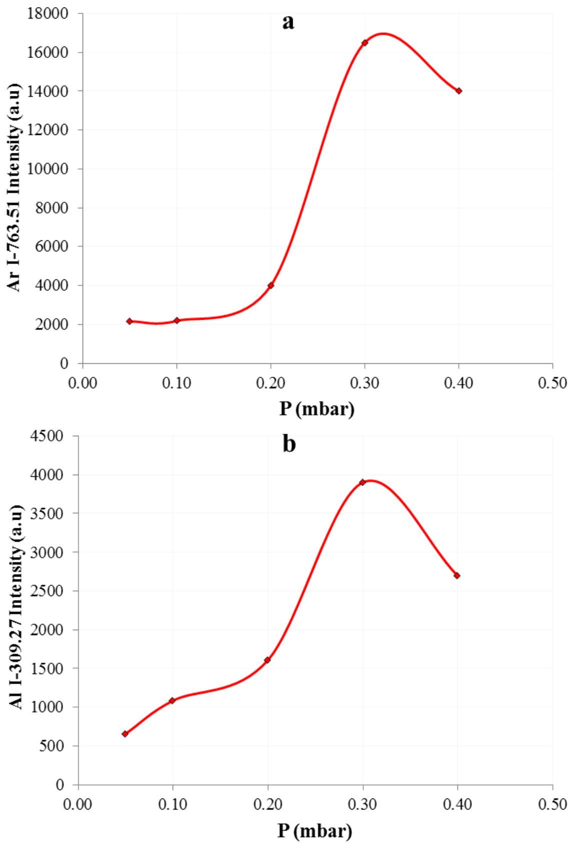

Fig. (4) Variation of intensity with working pressures for (a) Ar-I (763.51 nm) and (b) Al I (309.27)

Figure (4) illustrates the variation in emitted line intensities of Ar I (763.51 nm) and Al I (309.27 nm) in response to working pressures. The variation of line intensity for the discharge gas atoms indicates the excitation process within plasma and plasma density, which appeared at its optimum point at 0.3 mbar pressure as a result of increasing the probability of the excitation process. However, at high pressure with a high collision rate, there is insufficient path for electrons to attain the required energy for the ionization process. The intensity of the line corresponding to the Al line increased at 0.3 mbar pressure but decreased at 0.4 mbar pressure, enhancing the sputtering efficiency at the optimum point of 0.3 mbar. More sputtered atoms within the gas phase increased the probability of electron atom collision, which increased the excitation process and yielded more emitted photons, i.e., more intensity.

Figure (5) shows the variation in emitted line intensities of Ar I (763.51 nm) and Al I (309.27 nm) corresponding to the applied voltage at constant working pressures of 0.3 mbar. The curves demonstrate a direct relationship between line intensity and applied voltage for the sputtering gas and aluminum atoms. Increasing applied voltages results in more excellent acceleration of charged particles via electric force, contributing to enhanced plasma emission as a result of increasing the electrons' energy, causing more excitation and ionization process of Ar. The Ar ions with more energy enhance sputtering efficiency through accelerated Ar ions that go onto the target. It is critical to operate within a limited range of applied voltage to achieve optimal sputtering performance, as excessive voltage can result in instability and undesirable properties in the deposited films [24].

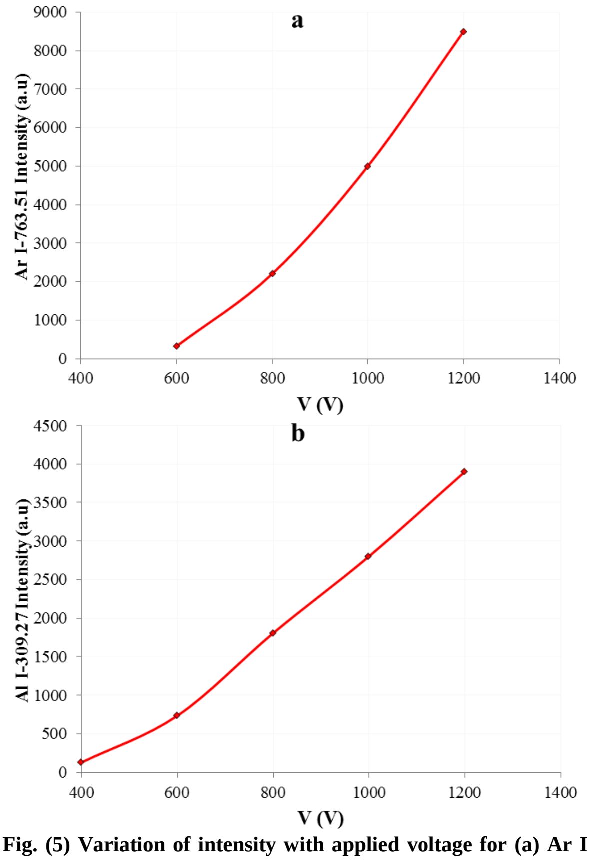

Fig. (5) Variation of intensity with applied voltage for (a) Ar I (763.51 nm) and (b) Al I (309.27)

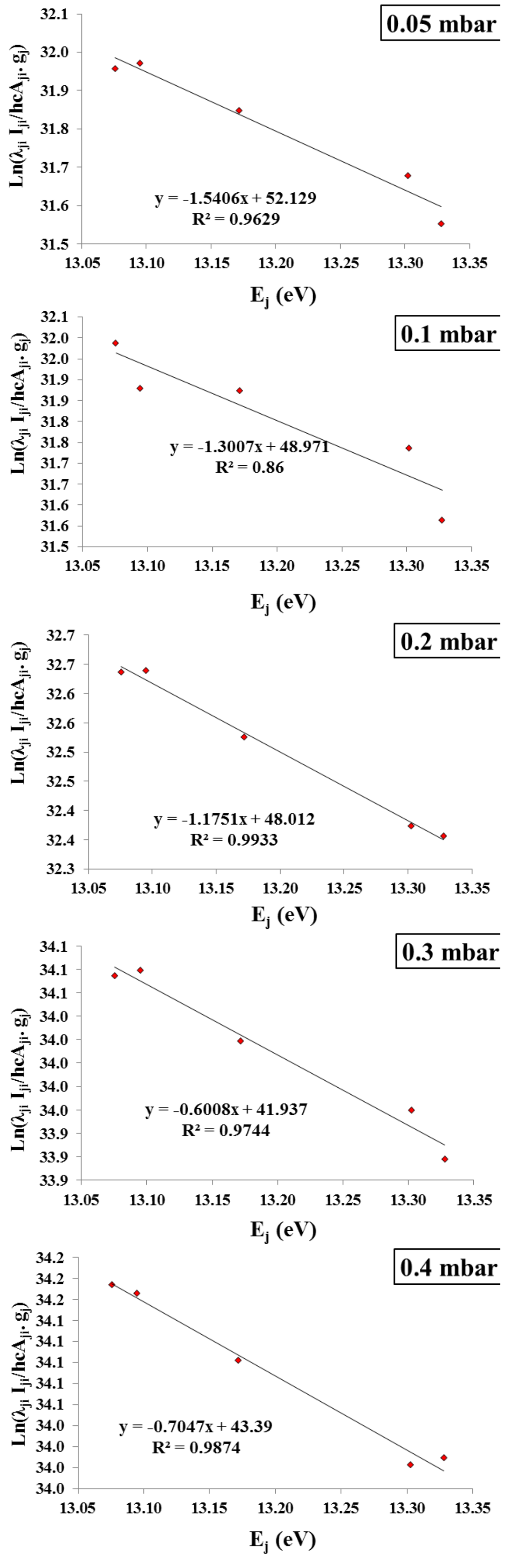

Fig. (6) Determination of plasma temperature at different working pressures and constant applied voltage of 1200 V, using Boltzmann-plot employing Al I lines

The electron temperature (T_e) at different sputtering conditions was determined by Boltzmann-Plot for plasma induced at different working pressures and different applied voltages, using atomic emission lines of aluminum, as shown in figures (6) and (7), respectively. T_e equals the inverse of slope values of the linear plot of $\ln(\lambda_{ji}\, I_{ji} / hcA_{ji}.\, g_j)$ against the energy of upper-level (E_j). Note that calculations were not performed at 500 V due to the low intensity of the spectral lines and not being recognized.

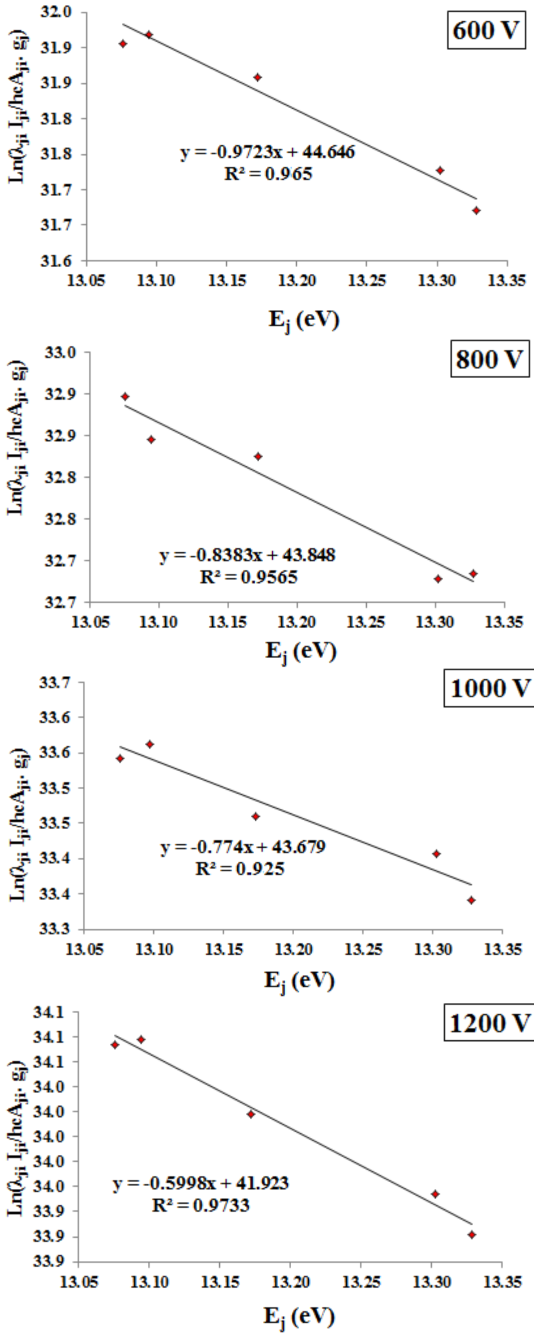

Fig. (7) Boltzmann plot for Al I lines at different applied voltages and constant working pressures of 0.3 mbar

Figures (8) and (9) depict Lorentzian fit for the Ar I (763.51 nm) emission line for DC sputtering from the Al target at different working pressures and applied voltages. The behavior of the emission line and its broadening concerning working pressure is intricate. It is evident that line broadening increases up to 0.3 mbar pressure and then decreases with increasing working pressure. This phenomenon is ascribed to fluctuations in plasma density, reaching an optimum pressure of 0.3 mbar, as discussed in previous sections. On the other hand, a direct correlation is observed between applied voltage and line broadening, which is attributed to an increase in electron number density, indicating a significant effect of voltage on the plasma's characteristics. The formed sheaths around ions at high electron density induce an electric field that causes line broadening.

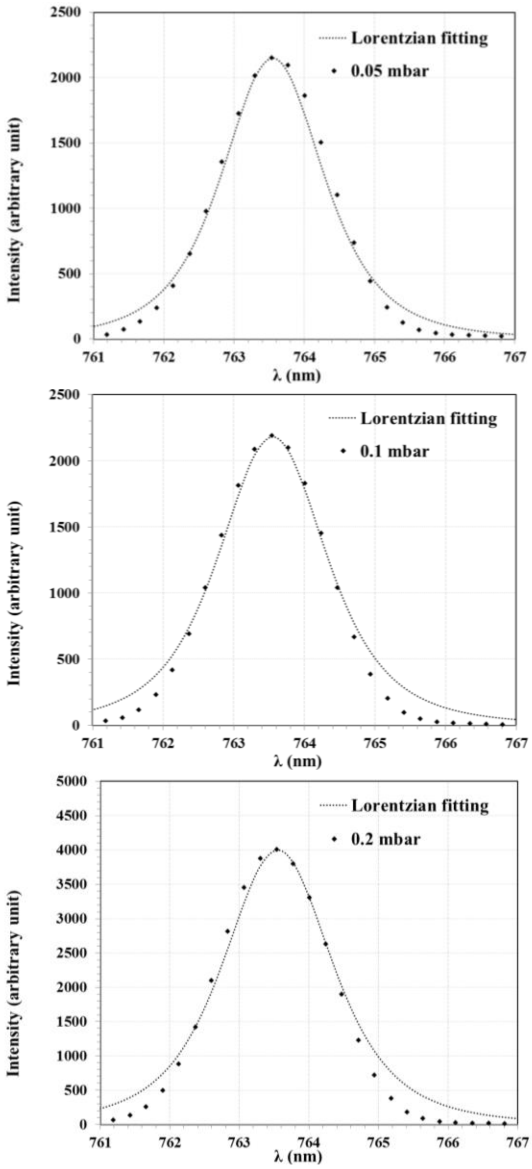

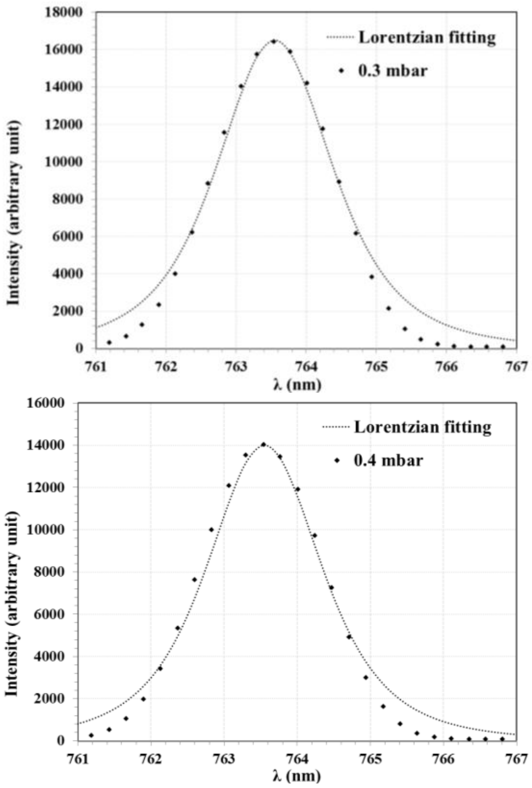

Fig. (8) Lorentzian fit for the 763.5 nm Ar-I during sputtering at different pressures and fixed applied voltage of 1200 V

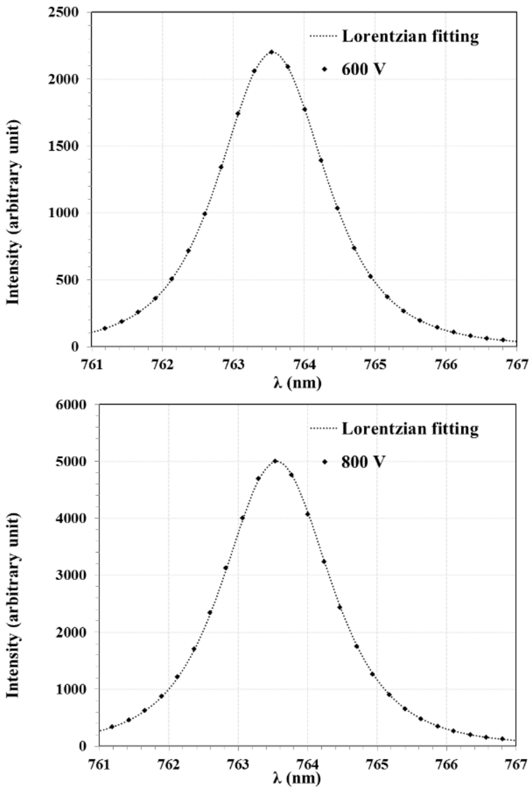

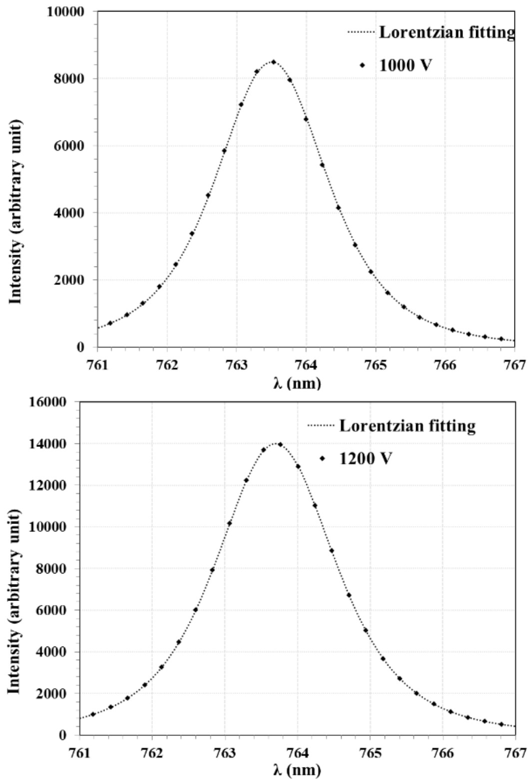

Fig. (9) Lorentzian fit for the 763.5 nm Ar-I during sputtering at different applied voltages and constant vacuum pressure of 0.3 mbar

Figure (10) illustrates the variation of electron temperature and electron number density with the working pressure and applied voltage in Argon discharge. Figure (10a) displays the maximum values of T_e and n_e at 0.3 mbar working pressure. At lower pressure levels, electrons can travel longer distances before colliding, as different types of inelastic collisions lose some of their energy. So, the electrons have a low number density and energy at this level. Consequently, more emissions are produced with the increasing pressure to reach their optimal value [25]. However, both T_e and n_e increased directly with the increase in applied voltage due to increasing the energy delivered to electrons by the higher electric field causing more ionization collision donate more electron to plasma.

Table (1) lists the plasma parameters of the breakdown across Ar by the DC sputtering system using the Al target at different applied voltages and working pressures. The trend of T_e and n_e variation with changing vacuum pressures increased with increasing working pressure from 0.05 to 0.3 mbar, while, at 0.4 mbar, T_e and n_e exhibited a decrease. This phenomenon can be attributed to increased electron-atom ionization collisions at specific pressures, leading to an elevation in n_e. Further increases in pressure beyond the optimal value reduced both T_e and n_e due to intensified collisions and energy transfer within the plasma. A direct relationship was observed between T_e and n_e with the applied voltage. The plasma parameters fulfill the plasma criterion as high plasma frequency, short Debye length, and a large Debye number.

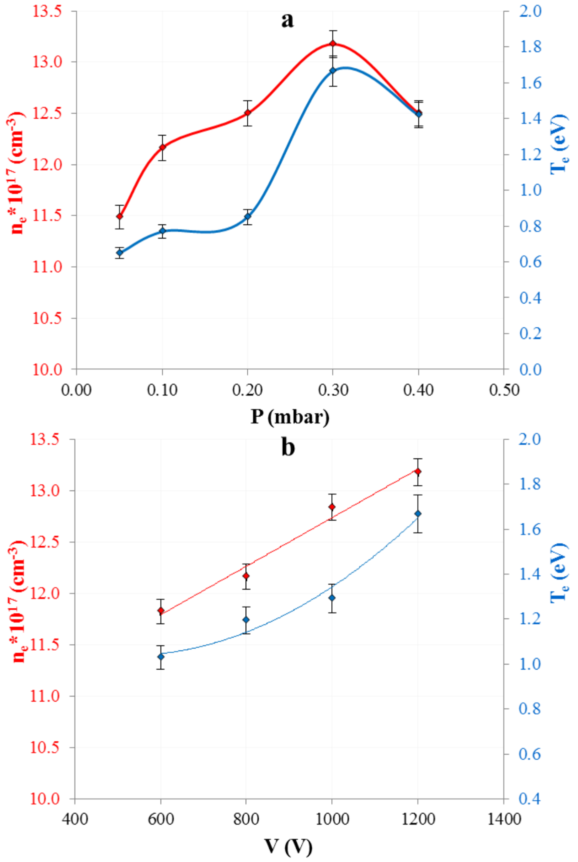

Fig. (10) Variation of n_e and T_e corresponding to working pressure (a) and applied voltage (b)

A shorter Debye length indicates a more efficient screening of the electric fields. As a result, a shorter λ_D could produce more energetic ions and affect the sputtering rate. The plasma frequency correlated to the square root of the electron number density, so it has the same variation behavior with its optimal value at 0.3 mbar vacuum pressure. It seems that λ_D increased with increasing applied voltage and has a maximum value at 0.3 mbar pressure. The sputtering rate is affected by the trajectories and energies of positive ions due to the presence of the Debye sheath, which is related to the electron Debye length [26]. A shorter Debye length forms a locally dense plasma near the cathode. So, ions reach the cathode and are accelerated by the sheath, enhancing the cathode's sputtering [27]. Therefore, a shorter λ_D enhances the sputtering rate [28].

4. Conclusions

The effects of working pressure and applied voltage on plasma discharge characteristics in argon using an aluminum target in a DC magnetron sputtering system were investigated using the OES technique. The results show a clear association between operational conditions and plasma parameters. These variations can be noticed using emission intensities corresponding to each species, which indicate sputtering efficiency. The results showed that the optimal operating vacuum pressure was 0.3 mbar. The emission intensity of both the sputtering gas and the metal atoms was at its maximum intensity at this pressure, which indicated a higher plasma density and more sputtered atoms in the gas phase, which showed an increase in the sputtering process. The intensity of the Ar-I and Al-I species' emitted lines increased with the applied voltage due to the increased energy supplied to the charged particles, which enhanced the probability of ionizing and excitatory collisions, increasing the emission lines' intensity. Moreover, other plasma parameters, including n_e, T_e, λ_D, f_p, and N_D, were found to change significantly with the change of vacuum pressure and applied voltage. These parameters significantly affect the efficiency of the sputtering process and thin film properties.

References

[1] L. Hultman "Surface & Coatings Technology Toward energy-efficient physical vapor deposition : Routes for replacing substrate heating during magnetron sputter deposition by employing metal ion irradiation", *Surf. Coatings Technol.*, 415 (2021).

[2] W.N. Raja et al., “Magnetic Field Distribution of Closed-Field Unbalanced Dual Magnetrons Employed in Plasma Sputtering Systems”, *Iraqi J. Appl. Phys.*, 12(3) (2016) 35-42.

[3] W.N. Raja et al., “Employment of Magnetron to Enhance Langmuir Probe Characteristics of Argon Glow Discharge Plasma in Sputtering System”, *Iraqi J. Appl. Phys.*, 12(4) (2016) 19-28.

[4] C. Deshpandey et al., "Preparation and properties of Al_2O_3 films by d.c. and r.f. magnetron sputtering", *Thin Solid Films*, 96(3) (2021) 127120.

[5] O.A. Hammadi et al., “Fabrication of UV Photodetector from Nickel Oxide Nanoparticles Deposited on Silicon Substrate by Closed-Field Unbalanced Dual Magnetron Sputtering Techniques”, *Opt. Quantum Electron.*, 47(12) (2015) 3805-3813.

[6] M.M. Shehab et al., "Spectroscopic diagnosis of the CdO:CoO plasma produced by Nd:YAG laser", *Iraqi J. Sci.* 62(9) (2021) 2948–2955.

[7] R.K. Jamal et al., "Designing A zener diode using $Ag_2O_{(1-X)}Zno_{(X)}$/PSi structures deposited by laser induced plasma technique", *Iraqi J. Sci.*, 61(5) (2020) 1032–1039.

[8] R.S. Mohammed et al., "Spectroscopy Diagnostic of Laser Intensity Effect on Zn Plasma Parameters Generated by Nd:YAG Laser", *Iraqi J. Sci.* 63(9) (2022) 3711–3718.

[9] S.N. Mazhir et al., "Cytotoxic activity of green zinc

selenide nanoparticles against Hep-G2 cell lines", *Indian J. Forensic Med. Toxicol.*, 15(1) (2021) 2072–2078.

[10] M.K. Khalaf et al., “Fabrication and Characterization of UV Photodetectors Based on Silicon Nitride Nanostructures Prepared by Magnetron Sputtering”, *Proc. IMechE, Part N, J. Nanomater. Nanoeng. Nanosys.*, 230(1) (2016) 32-36.

[11] M.K. Khalaf et al., “Silicon Nitride Nanostructures Prepared by Reactive Sputtering Using Closed-Field Unbalanced Dual Magnetrons”, *Proc. IMechE, Part L, J. Mater.: Design Appl.*, 231(5) (2017) 479-487.

[12] A. Sergievskaya et al., "Magnetron sputter deposition of silver onto castor oil: The effect of plasma parameters on nanoparticle properties, Colloids Surfaces A Physicochem", *Eng. Asp.*, 615 (2021) 126286.

[13] N.A.K. Jadoon et al., "Recent Advances in Aluminum Nitride (AlN) Growth by Magnetron Sputtering Techniques and Its Applications", *Inorganics*, 12 (2024) 264.

[14] R.T. Ahmed et al., "Influence of laser energy on structural and morphology properties of CdO and CdO:Sn production by laser-induced plasma", *J. Optics (India)*, 53(2) (2024) 1564–1573.

[15] X. Lu et al., “Reactive species in non-equilibrium atmospheric-pressure plasmas: Generation, transport, and biological effects”, *Phys. Rep.*, 630 (2016) 1-84.

[16] J. Held et al., "Ionization of sputtered material in high power impulse magnetron sputtering plasmas - comparison of titanium , chromium and aluminum", *Plasma Sources Sci. Technol.*, 32 (2023) 065006.

[17] D.V Sidelev et al., "Aluminum films deposition by magnetron sputtering systems : Influence of target state and pulsing unit", *J. Phys.*, 741 (2016) 012193.

[18] S. Muhl et al., "Aluminium nitride films prepared by reactive magnetron sputtering", *J. Phys. D: Appl. Phys.*, 30 (1997) 2147–2155.

[19] R. Wang et al., "Influence of Target Current on Structure and Performance of Cu Films Deposited by Oscillating Pulse Magnetron Sputtering", *Coatings*. 12 (2022) 394.

[20] Y.Z. You et al., "Influence of incidence angle and distance on the structure of aluminium nitride films prepared by reactive magnetron sputtering", *Thin Solid Films*, 515 (2007) 2860-2863.

[21] S. Venkataraj et al., "Structural, optical and mechanical properties of aluminium nitride films prepared by reactive DC magnetron sputtering", *Thin Solid Films*, 502 (2006) 235-239.

[22] M.O. Salman et al., "Comparison between plasma distribution in plane and concave cathodes DC discharge systems", *J. Theor. Appl. Phys.*, 18 (2024) 1-9.

[23] K.A. Aadim, "Optical emission spectroscopic analysis of plasma parameters in tin–copper alloy co-sputtering system", *Opt. Quantum Electron.*, 48(12) (2016) 545.

[24] C. Duquenne et al., "Thermal conductivity of aluminium nitride thin films prepared by reactive magnetron sputtering", *J. Phys. D: Appl. Phys.*, 45 (2012) 015301.

[25] S.N. Rashid et al., "Synthesized Zinc Nanoparticles via Pulsed Laser Ablation: Characterization and Antibacterial Activity", *Karbala Int. J. Mod. Sci.*, 8(3) (2022) 462-476.

[26] M. Makówka et al., "Correlation between plasma parameters and structure of thin TiO_2 films deposited by conventional and pulsed magnetron sputtering methods", *Appl. Surf. Sci.*, 578 (2022) 151808.

[27] S.M. Rossnagel et al., "Magnetron sputtering", *J. Vac. Sci. Technol. A*, 38 (2020) 060805-1-7.

[28] E. Koushki et al., "Oxygen amount effect on optical properties of aluminium oxide nanostructured films prepared by reactive magnetron sputtering", *Optik*, 127 (2016) 4635–4638.

Table (1) Variation of plasma parameters of the DC sputtering with working pressures and applied voltages

p (mbar)	V (V)	T_e (eV)	Δλ (nm)	$n_e \times 10^{18}$ (cm^{-3})	$f_p \times 10^{12}$ (Hz)	$\lambda_D \times 10^{-6}$ (cm)	N_D
0.05		0.649	1.700	1.149	9.624	5.585	838
0.10		0.769	1.800	1.216	9.903	5.907	1050
0.20	1200	0.851	1.850	1.250	10.040	6.130	1206
0.30		1.665	1.950	1.318	10.308	8.351	3215
0.40		1.376	1.850	1.250	10.040	7.794	2479
	600	1.029	1.750	1.182	9.765	6.930	1648
0.3	800	1.193	1.800	1.216	9.903	7.358	2030
	1000	1.292	1.900	1.284	10.175	7.454	2227
	1200	1.665	1.950	1.318	10.308	8.351	3215

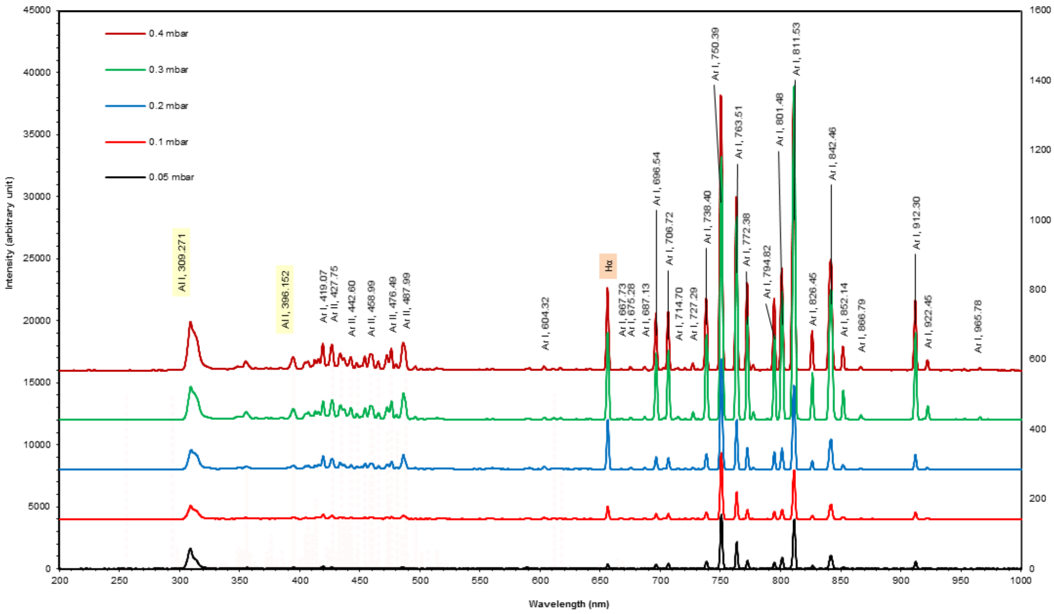

Fig. (2) Emitted spectra from DC sputtering system in Ar under different vacuum pressures using Al target

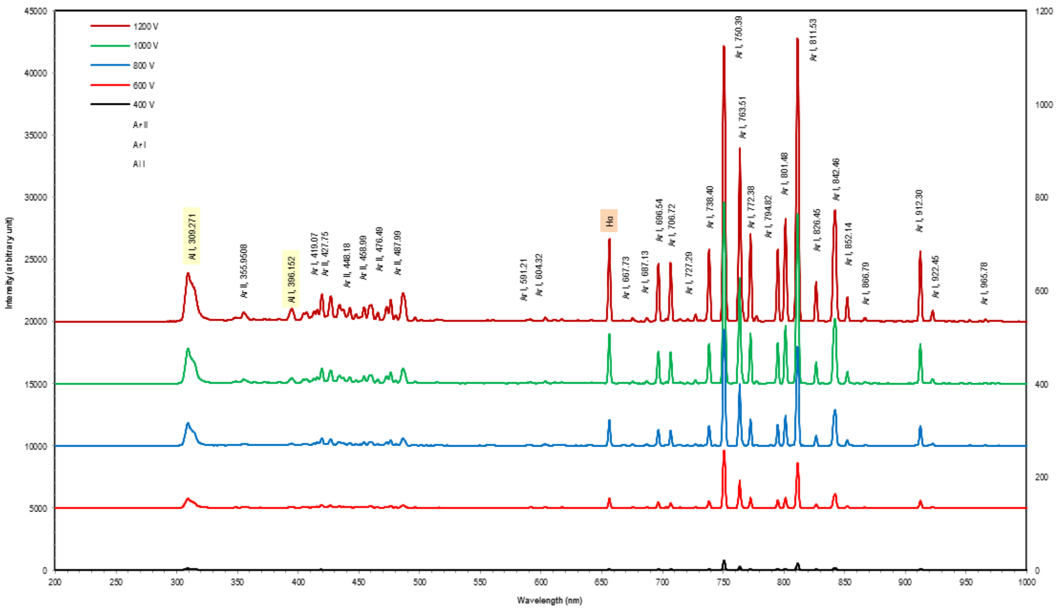

Fig. (3) Spectra of Ar discharge in DC sputtering system by different applied voltages using Al target

